*Ecological Applications,* 7(3), 1997, pp. 1039–1053

# MONITORING PACIFIC COAST SALT MARSHES USING REMOTE SENSING

M. ZHANG,[1] S. L. USTIN,[1,3] E. REJMANKOVA,[2] AND E. W. SANDERSON[1]

[1]*Department of Land, Air and Water Resources, University of California, Davis, California 95616 USA*
[2]*Division of Environmental Studies, University of California, Davis, California 95616 USA*

*Abstract.* The rapid decline in the extent and health of coastal salt marshes has created a need for nondestructive methods for evaluating the condition of salt marsh ecosystems. This paper describes simultaneous uses of field sampling and remote sensing approaches to understand salt marsh ecosystem functions and species distributions and discusses the implications for salt marsh monitoring using remote sensing. Three sites along the Petaluma River near the entrance into San Pablo Bay, California, which represented a range of soil salinity, water content, and nutrients, were studied. Standing biomass was directly assessed by field sampling and indirectly estimated through canopy reflectance. The sites were dominated by almost monotypic stands of *Salicornia virginica, Spartina foliosa,* and *Scirpus robustus.* For *Salicornia*, we found a positive relationship between salinity and biomass up to a threshold of 42 g/kg, after which biomass declined monotonically with increasing salinity. No *Scirpus* or *Spartina* were found at soil salinities >20 g/kg. Although significantly different levels of nitrate and ammonium nitrogen were found in the interstitial water and soils at these sites, no strong relationships were found between biomass and nitrate nitrogen. Soil ammonium nitrogen, in contrast, was positively related to biomass. Soil redox and salinity increased with elevation and distance from the shoreline, while soil moisture and $H_2S$ decreased. Canopy biomass was estimable using remotely sensed spectral vegetation indices at 58–80% accuracy depending on species. Simple Vegetation Index (VI) and Atmospherically Resistant Vegetation Index (ARVI) measured by handheld field spectrometers were the best estimators of green biomass for high cover of *Salicornia.* Soil Adjusted Vegetation Index (SAVI) and Soil Adjusted and Atmospherically Resistant Vegetation Index (SARVI) gave the best estimates for *Spartina* while the Global Environment Monitoring Index (GEMI) was the best estimate for *Scirpus.* The relationships between vegetation indices and biomass were developed from field spectra. The VI was used to estimate spatial patterns of biomass across the salt marsh from Landsat satellite Thematic Mapper (TM) data. The TM image showed spatial patterns corresponding with species zones and biomass abundance. Narrow band reflectance features measured with a handheld spectrometer can be used to predict canopy plant water content ($R^2 = 63\%$). Interpolated estimates of water content from field-measured canopy reflectance were shown to relate to variation in salinity and soil moisture. Canopy water content was estimated from Airborne Advanced Visible Infrared Imaging Spectrometer data, which showed similar spatial patterns at the site. Results indicate that both biomass production and canopy water content can be accurately determined from remotely sensed spectral measures. Species-specific differences in these characteristics may be used for monitoring species distribution and abundance from airborne or satellite images.

*Key words: ammonium nitrogen; biomass; canopy water content; environmental monitoring; hydrogen sulfide; interstitial water; nitrate nitrogen; redox; remote sensing; salinity; salt marsh; spectral vegetation index.*

## INTRODUCTION

Salt marshes have been subject to extensive exploitation, modification, and destruction. Loss of marshes is a topic of great concern because salt marshes provide essential functions in the buffering and transfer of energy and nutrients and maintenance of estuarine water quality (Odum 1983). Productivity of salt marshes is a primary indicator of ecosystem health (Leibowitz and Brown 1990), but biomass production is difficult to estimate accurately given the heterogeneity and large spatial gradients within salt marshes. The inherent heterogeneity within these systems and the difficulty for direct access supports the need for broad-scale remote monitoring techniques.

The next generation of earth-observing satellites will include sensors having many additional spectral channels and higher spatial resolution, which offer new opportunities to provide information about site conditions. The purpose of this study was to examine the edaphic factors controlling growth and biomass and to determine the extent of detection of these differences in canopy reflectance using broad-band vegetation in-

Manuscript received 22 September 1995; revised 26 July 1996; accepted 12 September 1996; final version received 4 November 1996.

dices related to absorption by photosynthetic pigments or a narrow-band spectral feature related to canopy water absorption. We wish to test the applicability of using remotely sensed vegetative indices for differentiation and condition of coastal marshes.

Pacific coast tidal marshes are dominated by perennial species such as *Salicornia virginica, Spartina foliosa, Scirpus robustus, Jaumea carnosa, Frankenia salina, Triglochin maritimus,* and *Limonium californicum* (Ibarra-Obando and Poumian-Tapia 1992). Of these, *Salicornia virginica, Spartina foliosa,* and *Scirpus robustus* are the most common representatives in the San Pablo Bay estuary, the northern extent of San Francisco Bay, California (Atwater et al. 1980), with *Salicorina* providing ≈90% cover. These species have very different canopy architectures and adaptive mechanisms to cope with salinity, and these attributes provide a basis for their remote detection and identification. Specifically, differences in leaf angle distribution, leaf and stem density, succulence, and the amount of canopy litter create canopies having different spectral features that should permit their unique identification.

A general understanding of the physiological factors maintaining salt marsh structure and community distributions and biomass is known, the result of complex interactions among sedimentation rates, freshwater and tidal influxes, tidal changes, and weather patterns (Mahall and Park 1976, Atwater et al. 1980, Ustin et al. 1982, Whitlow 1982, Zedler 1983, Pearcy and Ustin 1984, Bertness and Ellison 1987, Deleeuw et al. 1990). Typically, proximity to drainage canals and microtopography within the marshes control these relationships (Hager and Schemel 1992) and create a complex spatial mosaic.

Thus, despite the general understanding of factors controlling biomass production, it remains difficult to extrapolate spatial patterns of biomass production and species distributions from a few sample points even with accurate measurements because of the extreme edaphic heterogeneity within salt marshes where only a few centimeters elevational change creates dramatically different conditions in salinity, nutrients, redox potential, pH, and soil moisture. While field observations have shown excellent relationships between plant response and salt marsh chemistry, the spatial and temporal variations and inaccessibility of the salt marsh make mapping large areas relatively difficult (Gross et al. 1989). Remote sensing provides a means for understanding large-scale vegetation patterns and dynamics (Roughgarden et al. 1991). Species having greatly different leaf and branching angle geometries can be separated in reflectance data as reviewed by Goel (1988). Gross et al. (1989, 1993) have taken advantage of these canopy differences using a vegetation index developed from the ratio of near-infrared to red reflectance derived from satellite data to map vegetation distributions. Klemas et al. (1993) reported a simplified coastal land cover classification system designed for satellite data. Even though biomass has been estimated using the vegetation index for some salt marsh species, the appropriate choice of vegetation indices or application of other hyperspectral models that could be developed with the next generation of multichannel sensors has not been fully examined in salt marshes (Gross et al. 1989). Despite numerous studies, relationships between reflectance and vegetation canopy characteristics still tend to be site or condition specific.

Vegetation indices derived from satellite and/or handheld spectrometer-based are frequently used to estimate net primary production and monitor the vegetation phenologic patterns (Lozano-Garcia et al. 1991, Christensen and Goudriaan 1993). Much effort has been made toward using simple vegetation indices (VI) based on ratios or the Normalized Difference Vegetation Index (NDVI) to estimate wetland biomass production, differentiate wetland species, and map species distributions (Drake 1976, Hardisky et al. 1983, 1986, Gross and Klemas 1986, Gross et al. 1989, 1993). Vegetation indices are based on the difference in absorption of electromagnetic energy in the red and the near-infrared by chlorophyll. Red light is strongly absorbed by the upper layers of the canopy while near-infrared flux is reflected out of the canopy, and some studies have shown that VI and NDVI are proportional to the absorbed photosynthetically active radiation (APAR) (Baret and Guyot 1991, Myneni and Williams 1994). The NDVI often provides better estimates than VI because it accounts for albedo variations, which may confound canopy differences.

More recently, new indices have been developed that improve the vegetation index (Baret and Guyot 1991, Huete et al. 1994) by minimizing the contribution of soil variation and atmospheric scattering, which might provide better measures for wetland conditions. These include the Soil Adjusted Vegetation Index (SAVI, Huete 1988), which is designed to eliminate soil-induced variation and is useful where soil backgrounds differ and low canopy cover is present. The Atmospherically Resistant Vegetation Index (ARVI, Kaufman and Tanre 1992) minimizes atmospheric-induced variations making the vegetation index less sensitive to temporal and spatial variations in atmospheric aerosol content. The Global Environment Monitoring Index (GEMI, Pinty and Verstraete 1992) is another method that minimizes atmosphere-induced variations in the vegetation index (Pinty and Verstraete 1992). The GEMI index also provides greater sensitivity to changes in biomass at high levels of biomass. The Soil Adjusted and Atmospherically Resistant Vegetation Index (SARVI, Huete et al. 1994) attempts to simultaneously minimize both soil and atmospheric variations and is reported to provide a more stable vegetation index to estimate biomass production (Huete et al. 1994).

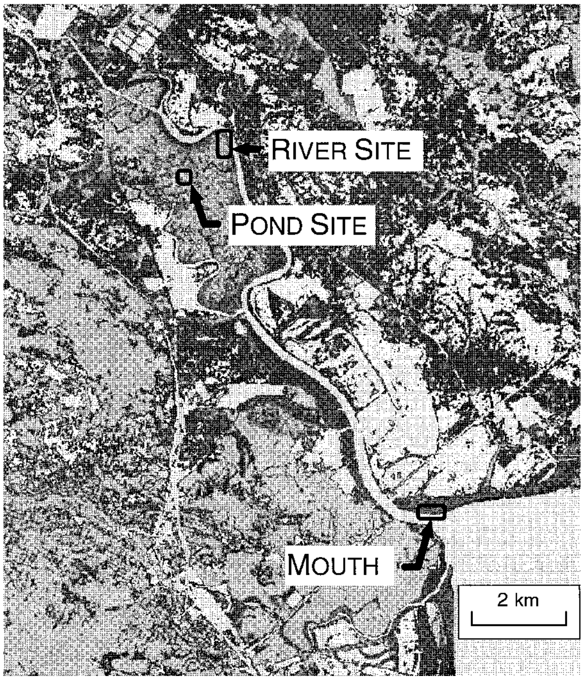

FIG. 1. Location of study areas along the Petaluma River and San Pablo Bay, California. Figure is part of a TM scene obtained on 20 June 1990. Pixel resolution is 30 m, and a scale bar is shown for reference. Marshes are continuous along the shoreline and river margin and widen into a large brackish marsh in the vicinity of the Pond and River sites. The surrounding area is primarily dryland farming, and differences in land use are apparent. The image displayed is the vegetation index (VI), a ratio of band 4 to band 3; brighter values indicate higher biomass, and darker values indicate low biomass. The image was thresholded such that water (which normally has near 0 values) is displayed as gray to give the marshes along the river margin maximum contrast.

## MATERIALS AND METHODS

### *Study area*

Three sites in the salt marshes along the Petaluma River and the entrance into San Pablo Bay, California were selected for study (Fig. 1). A portion of a Landsat Thematic Mapper satellite image, 14 by 12 km, acquired on 20 June 1990, ≈0945 Pacific Standard Time (PST) depicts the northern shoreline of San Pablo Bay estuary, Petaluma River, and surrounding area. The Thematic Mapper satellite image of the San Pablo Bay region was created from a ratio of band 4/band 3 (red/near-infrared reflectance), and a linear gray scale stretch was applied to enhance spatial variation in the Petaluma River salt marsh. The sites are identified in the figure as Mouth, Pond, and River. The Mouth site is located near the mouth of the Petaluma River. The River and Pond sites are located ≈10 km inland from the shore of San Pablo Bay. These relatively undisturbed sites were chosen because they represented the range of salinity, nutrient, and hydrologic conditions for San Pablo Bay tidal salt marshes. Field measurements were made in May and June 1994 to coincide with peak spring growth.

### *Field measurement design and data collection*

Three different site conditions were studied. Various sized grids and transects were used for locating sampling points because of differences in site geometry and conditions among study sites. Both biological and spectral data were collected at geo-located grid points. The differentially corrected Universal Transverse Mercator (UTM) coordinates were determined using a Trimble Navigation Pathfinder Basic Plus Global Positioning System (GPS) with a location accuracy of 2–5 m. The Trimble Navigation community base station located in Sunnyvale, California was used for differential correction.

At the Mouth site, exposed to the greatest tidal inundations and fluctuations, there was a relatively simple inland gradient from the shoreline. Channels were oriented normal to the shoreline. Therefore, ten parallel transects were set out along lines perpendicular from the shoreline to an interior levee. Ten sample points, sequenced as A (nearest to the shoreline), to J (near the interior levee) were selected along each transect. The distances between sampling points were closer between A to D (20 m) than the distances between E to J (30–40 m). The sampling interval was chosen based on the species distributions and the elevational gradient. The total site area sampled was ≈380 by 400 m within a strip marsh extending east along the bayshore several kilometers from the mouth of the Petaluma River. A subset of sampling points (B, C, D, G, and I) were sampled for biomass, salinity, redox, and nutrients in addition to canopy cover and spectral measurements. The Pond site was located ≈150 m interior from the banks of the Petaluma River, and experienced little tidal inundation. There were no obvious channels for interior water transport at the site and the gradient oriented radially outward from the ponds. Thus, at the Pond site eight transects (T to Z) were placed radiating outward from the pond, extending over a total area of 100 by 120 m. Alternating transects were sampled at distances of 0, 30, and 60 m from the ponds for biomass, salinity, redox, and nutrients. At the River site, a network of small channels dissected the area which, because of a major inlet from the river, has an inland gradient on two sides of the site. At this site (150 by 200 m), because of the greater spatial complexity, we placed a 15-m grid and sampled over the entire study area. Because of the smaller extent and the complex environmental gradient for salinity and nutrients, a third of all the points were selected following a stratified random sampling scheme for biomass, salinity, redox, and nutrients. All sampling points at all three sites were sampled for canopy cover, height, and canopy reflectance.

The aboveground biomass was sampled from circular (0.13-$m^2$) plots, which were determined by the field-of-view of the field spectrometer. The plot size was limited by the reach of the fiber optic cable above the canopy. After clipping, biomass was put into labeled plastic bags and then returned to the laboratory for processing. The samples were separated by species into green foliage, woody stems, and litter. Fresh mass was obtained within 24 h after harvest and the dry mass was obtained after oven drying for three or more days at 70°C. Leaf area was measured using a LI-COR (LI-3000A) leaf area meter (LI-COR, Incorporated, Lincoln, Nebraska, USA) for *Spartina* and *Scirpus*, and leaf area of *Salicornia* was estimated using a cone surface area formula and measures of fleshy stem diameter at both ends of the green shoots and the length. Leaf area index (LAI) for each species was calculated according to Norman and Campbell (1989). Canopy water content was estimated for each species as the difference between fresh and dry masses for each canopy component (leaves, stems, litter).

Soil redox potentials (Eh) at 30-cm depth were measured with four replicates with brightened platinum electrodes, which were allowed to equilibrate in situ for ≈20 min before measurement. The potential of a calomel reference electrode (+244) was added to each value to calculate Eh.

Soil samples were collected for gravimetric moisture, nutrient, and salinity analysis with a small trowel for the 0–15 cm depth because up to 75% of the roots occur within the upper 15-cm depth in these marshes (Mahall and Park 1976, Ustin et al. 1982, Whitlow 1982). Soils were air dried, sieved, and analyzed for conductivity and pH using a 1:3 soil : water solution. Total nitrogen was determined on a Perkin Elmer 2400 CHN analyzer. $NO_3$-N and $NH_4$-N were analyzed according to Allen (1989).

Interstitial water was collected using a sampler described by McKee et al. (1988) that consisted of a perforated plastic pipette with a sealed lower end connected to a 50-mL syringe, permitting collection of soil water at different depths. For hydrogen sulfide analysis, the first 5–10 mL of each sample was discarded and the subsequent 20 mL of water was transferred into a plastic centrifuge tube containing an equal volume of an antioxidant buffer. The buffer prevented the oxidation of sulfide and converted $H_2S$ and $HS^-$ forms of sulfur to $S^{-2}$. An additional 30 mL of interstitial water was transferred into a Nalgene bottle and saved for other nutrient analyses. Total sulfide was analyzed using ORION silver/sulfide ion-selective electrode and ORION 530 meter (Orion Research Incorporated, Boston, Massachusetts, USA). The remaining water samples were filtered through GF filters and analyzed for $NO_3$-N and $NH_3$-N according to Allen (1989).

Canopy spectra, canopy cover, and canopy height were collected at every sampling point at each of the three locations. Percentage canopy cover was estimated visually from the 0.13-$m^2$ plots. Canopy spectra were measured using a field portable spectrometer, Analytical Spectral Devices (ASD) Personal Spectrometer II (Analytical Spectral Devices, Boulder, Colorado, USA) with 1.45-nm sampling interval and spectral wavelength ranging between 350 and 1060 nm. Measurements were made in the nadir orientation with an 18° field-of-view restrictor at 1 m above the canopy (the projected area at canopy height was 0.13 $m^2$). At each sample point, five spectra were averaged. Spectra were calibrated to apparent surface reflectance by ratioing spectra to a horizontally leveled Spectralon panel 99% reflective ceramic material (Labsphere, Incorporated, North Sutton, New Hampshire, USA), measured before and after each set of five spectra. Spectra were measured within ±3 hour solar noon to reduce solar angle effects.

Although ideal procedures would have further minimized sun angle changes in field-collected spectra, limited access in the marsh because of high tide cycles dictated spectral collection over a 6-h period. Simple comparison between spectral reflectances showed that differences in reflectance were nearly zero in the visible range between 400 and 660 nm wavelengths and were <2.6% in the near-infrared wavelengths between 700 and 1060 nm for *Spartina* for samples taken on two separate days at 0918 and 1507 PST. The largest reflectance difference (<4%) was found for *Salicornia*, for samples taken at 1402 and 1630 PST. Cover was highest in this species and reflectance differences are not attributable to variations in background moisture, but to the variation within the species canopy.

Two integration times were used to capture the best signal-to-noise for both visible and infrared wavelength regions of the spectrum. This step was necessary because of the poor sensitivity of the silicon detector at wavelengths >800 nm. Because the joined segments had a misalignment in reflectance and some noise in the infrared spectrum at wavelengths longer than 800 nm, a moving standard deviation was calculated for every nm, using a 10 nm wavelength interval, to smooth reflectance and minimize noise in the infrared region.

### *Spectral analysis methods*

The wavelength intervals matching the Thematic Mapper (TM) bands were generated from the field-measured canopy reflectance data and vegetation indices (VI, NDVI, SAVI, GEMI, ARVI, SARVI) and were calculated using TM band 1 (450–520 nm), TM band 2 (520–600 nm), TM band 3 (630–690 nm), and TM band 4 (760–900 nm). Table 1 provides the formulas for calculating these indices and their citations.

An absorption feature is caused by the molecular absorption of energy and is observed in the spectrum as a depression of the reflectance across a specific wavelength interval. The continuum removal technique computes the difference in reflectance between the absorption feature and the spectral continuum over the wavelength interval spanning the feature. The reflectance across the interval is the shape of the spectrum

TABLE 1. Definitions of vegetation and soil spectral indices.

| Index | Description | Definition | Source |
|---|---|---|---|
| VI or SR | Simple Ratio of Vegetation Index | $p_n/p_r$ | Pearson and Miller 1972 |
| NDVI | Normalized Difference Vegetation Index | $(p_n - p_r)/(p_n + p_r)$ | Rouse et al. 1974 |
| SAVI | Soil Adjusted Vegetation Index | $[(p_n - p_r)/(p_n + p_r + L)](1 + L)$, $L = 0.5$ | Huete 1988 |
| GEMI | Global Environment Monitoring Index | $\eta(1 - 0.25\eta) - (p_r - 0.125)/(1 - p_r)$<br>$\eta = (2(p_n^2 - p_r^2) + 1.5p_n + 0.5p_r)/(p_n + p_r + 0.5)$ | Pinty and Verstraete 1992 |
| ARVI | Atmospherically Resistant Vegetation Index | $(p_n^* - p_{rb}^*)/(p_n^* + p_{rb}^*)$, $p_{rb}^* = p_r^* - \gamma(p_b^* - p_r^*)$ | Kaufman and Tanre 1992 |
| SARVI | Soil Adjusted and Atmospherically Resistant Vegetation Index | $(p_n^* - p_{rb}^*)/(p_n^* + p_{rb}^* + L)$ | Huete et al. 1994 |

*Note:* In the definitions, $p_r$ refers to the percentage reflectance in the red wavelength, $p_n$ refers to the percentage reflectance in the near infrared, and $p_b$ refers to the percentage reflectance in the blue band wavelength. An asterisk (*) means that these values were corrected by molecular scattering and ozone absorption.

in the absence of the narrow band absorption (Clark and Roush 1984). In the reflectance curve of vegetation, canopy water generates an absorption feature centered at 970 nm, with the depth of the absorption depending on the water content of the canopy. The estimate of absorption by liquid water was calculated as the area between the measured reflectance curve and the line connecting the reflectance points between 900 and 1040 nm. It is clear from the canopy reflectance data that variations in canopy spectra not only include bidirectional canopy characteristics, but also light scattered into the spectrometer from the surrounding surfaces. We adjusted for the local scattering effect by using $Y_i = (X_i - (X_{loc} - \bar{X})$, where $Y_i$ is the adjusted reflectance, $X_i$ is the actual measure of reflectance, $X_{loc}$ is average reflectance of a site, and $\bar{X}$ is the grand mean of all data.

To interpolate the field spectral data into an image for canopy water content, we took data from the Mouth site to illustrate the method and used the Inverse Distance Weighted (IDW) interpolation function in the ARC/Info GRID 7.03 (Environmental Systems Research Institute, Redlands, California) module with a 10-m grid size. We also compared the model with simple kriging functions in GRID. Because the standard deviation from the IDW was smaller (0.61) than from the kriging interpolation (0.81), and because the kriging program treats edge data as negatives, we present the IDW data. A simple comparison of other grid sizes (up to 30 m), indicated little dependence on scale for these patterns. Therefore, 10-m grid interpolation results were chosen to illustrate canopy water content patterns.

Spatial water content patterns are shown in the Advanced Visible Infrared Imaging Spectrometer (AVIRIS) image for the Mouth site, acquired 21 May 1994 near solar noon. The image was calibrated to surface reflectance using the ATREM program (CSES/CIRES, 1996). The NASA AVIRIS airborne sensor provides 224 contiguous 10-nm spectral channels covering the visible and reflected infrared region for each pixel. Nominal pixel resolution is 17.5 m. Landsat Thematic Mapper (TM) satellite image was acquired 20 June 1990 near 1000 PST. It has six spectral channels in the visible and reflected infrared region for each pixel. TM bands 3 (red) and 4 (near-infrared) were used. Nominal pixel resolution is 30 m. A regression relationship was established between the area under the continuum and the canopy water content following the analysis procedure described in the field spectra methods and more completely in Sanderson et al. (*unpublished manuscript*). In addition, general correlation and regression methods were used in the study for identifying relationships between variables and constructing statistical models. Pearson correlation coefficients were used to evaluate the relationships between field-measured vegetation indices and site characteristics. Statistics were performed using SAS (SAS 1990) statistical package.

## RESULTS

Point cover estimates show that *Salicornia* comprised 80% of the total sampled area and dominated the upper marsh while *Spartina* comprised 14% of the total sampling area and dominated the lower intertidal shoreline. *Scirpus* was 5% of the total area and was found in the zone between *Salicornia* and *Spartina* in discontinuous patches and at higher elevations within the marshes where lower salinities occur. *Scirpus* forms relatively sparse canopies at both Mouth and River sites but is locally abundant at other locations on the Petaluma River where it forms extensive monotypic stands growing on less saline sites. The zone occupied by *Spartina* is flooded during daily high tides, while the upland *Salicornia* is only flooded during the monthly high tides. The Mouth site experiences the greatest tidal fluctuations and had few channels in the interior of the marsh, while the River site has a dense network of channels and less tidal inundation. Lastly, the Pond site has infrequent tidal inundation and highest salinities. Standing water is present in several ponds that are below the elevation of the shallow water table but there are no obvious channels for interior water transport from the Petaluma River.

At the River site, eight species were collected with

TABLE 2. Species found in the Mouth, River, and Pond sites.

| Locations | Species | Frequency of occurrence among sampling points (%) |
|---|---|---|
| Mouth | *Salicornia virginica* | 80 |
| | *Spartina foliosa* | 30 |
| | *Scirpus robustus* | 2 |
| | *Jaumea carnosa* | 1 |
| | *Frankenia salina* | 1 |
| | *Distichlis spicata* | 2 |
| Pond | *Salicornia virginica* | 100 |
| | *Jaumea carnosa* | 3 |
| | *Frankenia salina* | 10 |
| River | *Salicornia virginica* | 79 |
| | *Spartina foliosa* | 10 |
| | *Scirpus robustus* | 14 |
| | *Jaumea carnosa* | 0.5 |
| | *Frankenia grandifolia* | 6 |
| | *Lepidium latifolium* | 1 |
| | *Baccharis pilularis* | 1 |
| | *Distichlis spicata* | 5 |

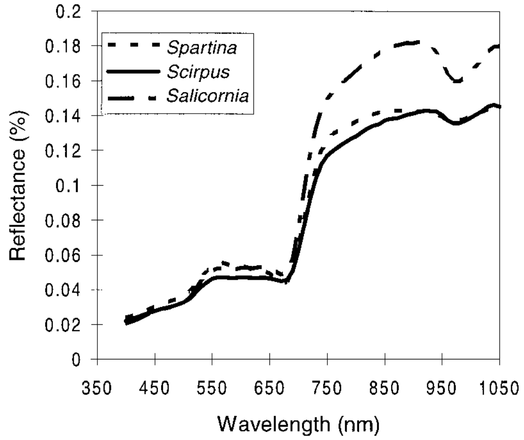

FIG. 2. Mean canopy spectral reflectances of three major salt marsh species (*Salicornia virginica, Spartina foliosa,* and *Scirpus robustus*) from all sites, June 1994.

high frequency of occurrence (Table 2). At the Mouth site six species had high frequency and at the Pond site three species were collected with lower frequency. These species mainly grow along the microchannels where salinities are less than in the intertidal regions farther removed from tidal flushing or on berms, levees, and elevated sites within the marsh. Lower salinities near the microchannels apparently encourage colonization by less salt-tolerant species, for which a greater number of species exist than more salt-tolerant species.

### *Spectra of the dominant species in the marsh*

Although the means for canopy spectra of these species were similar in shape and generally characteristic of vascular plants, *Salicornia* had the highest reflectance and *Scirpus* had the lowest reflectance over the spectrum (Fig. 2). *Salicornia* had a steeper slope and *Scirpus* had a lower slope in the red edge wavelength region (between 680 and 730 nm). *Spartina* was intermediate in its spectral features as shown in Fig. 2. As expected by differences in succulence, the canopy reflectance of *Salicornia* shows a deeper liquid water absorption feature at 970 nm when compared to *Spartina* and *Scirpus.* Standard errors of the mean are similar for the three species with *Scirpus* having the largest values across the spectrum, related to their smaller sample size. Standard errors are below 0.5% reflectance over the visible region and below 1% reflectance in the infrared.

Almost all the spectral indices (VI, NDVI, SAVI, GEMI, ARVI, and SARVI) derived from the field canopy spectra showed better relationships to green fresh mass biomass than to total harvested biomass, which included standing litter and dead foliage. Higher correlation coefficients were found between VI and green fresh mass ($r^2 = 0.58$) than other indices (Fig. 3). Although significant correlation coefficients were found for SAVI, SARVI, GEMI, and several canopy variables (Table 3), many of these relationships are not statistically significant at the 5% level. GEMI was better correlated with canopy height, soil salinity, redox, $H_2S$, and $NH_4$-N than other indices.

After separating spectral indices by species, we found SAVI and SARVI were positively related to dry mass in *Spartina* with the highest correlation coefficients while VI and ARVI correlated with green biomass in *Salicornia* (Table 4). Green biomass in *Scirpus* was best predicted using the GEMI. Correlation coefficients from ARVI are not statistically significant from VI, and likewise, the coefficients from SARVI are not statistically different from SAVI. These results were unexpected as the derived indices were presumed to provide more robust relations. Further separating spectral data for both location and species, similar correlations between the indices and biomass were found (Table 5). For *Spartina* at the River site, SAVI provides the best prediction of variation in dry green biomass.

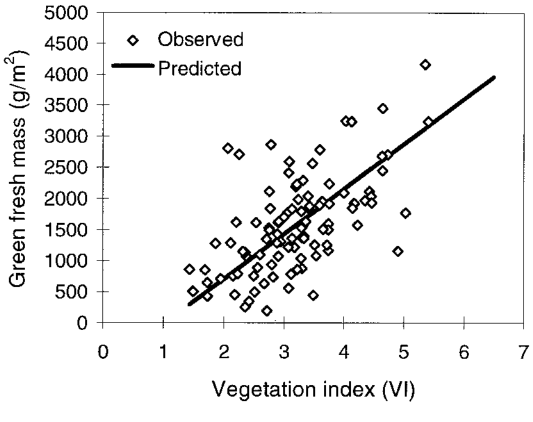

FIG. 3. The relationship between green fresh mass (g/m$^2$) and the vegetation index (VI) for salt marshes for all samples from all three sites in San Pablo Bay, California, June 1994 (green fresh mass [g/m$^2$] = $-742.6 + 723.4$ VI, with $R^2$ = 58.4%).

TABLE 3. Correlation coefficients ($r$) between the indices of field spectral measures and the measured biomass and environmental variables.

| Variable | $n$ | VI | NDVI | SAVI | GEMI | ARVI | SARVI |
|---|---|---|---|---|---|---|---|
| Total fresh mass | 109 | 0.59** | 0.51** | 0.54** | 0.46** | 0.56** | 0.55** |
| Green fresh mass | 109 | 0.72** | 0.57** | 0.58** | 0.49** | 0.71** | 0.62** |
| Total dry mass | 108 | 0.33** | 0.32** | 0.36** | 0.31** | 0.30** | 0.34** |
| Green dry mass | 108 | 0.58** | 0.48** | 0.54** | 0.49** | 0.59** | 0.58** |
| Mean canopy height | 109 | −0.23* | −0.26** | −0.49** | −0.54** | −0.15 | −0.41** |
| Salinity | 102 | ns | ns | 0.34** | 0.41** | ns | 0.22* |
| Redox | 111 | 0.25** | 0.34** | 0.41** | 0.41** | ns | 0.33** |
| Hydrogen sulfide | 95 | ns | ns | 0.44** | 0.56** | ns | 0.32** |
| $NH_4$-N in water | 100 | ns | ns | 0.42** | 0.53** | ns | 0.28** |
| $NH_4$-N in soil | 93 | ns | ns | 0.28** | 0.40** | ns | 0.15 |
| $NO_3$-N in water | 99 | 0.25* | 0.33** | 0.27** | 0.21* | 0.21* | 0.28** |
| $NO_3$-N in soil | 93 | ns | ns | ns | ns | ns | ns |

*Note:* See Table 1 for definitions of indices.
* $P < 0.05$; ** $P < 0.01$; ns = not significant.

After verifying that the VI relationships from the canopy spectra produced relatively high $r^2$, we produced a VI map of the salt marsh from a satellite TM image (Fig. 1). The image shows the magnitude of spatial variation in VI for the marsh and adjacent farmland. The marsh is continuous around the mouth of the Petaluma River and upstream several kilometers to the River and Pond sites. Although VIs are lower within the salt marsh than the highest values in the adjacent farmland, the values are clearly intermediate in range, more variable at a small scale, and show less sharp land-use discontinuities than the agricultural fields. Within the marsh, the Mouth site has generally lower VIs than the wetland near the River and Pond sites. Significant spatial variation in VIs within the sites is apparent, and at the scale displayed, associated with the larger channels and physical features.

### *Canopy water absorption continuum removal*

An analysis focusing on the water absorption feature at 970 nm was used to determine canopy water content for each species. The relationship to canopy water content is inferred by regressing the water absorption feature and the actual canopy water content. Sixty-three percent of the foliar variation in water content is explained by the water absorption feature (Fig. 4). *Spartina* has the lowest measured water content and smallest spectral estimates of water absorption. *Spartina* occupies the lower intercept in the regression scatter plot with absorption area values $<0.85$ kg/m$^2$ and with prediction certainty of $>70\%$. *Salicornia* has the highest water content, absorption values $>0.85$ kg/m$^2$, and the highest values on the regression line. *Salicornia* samples also showed the greatest variation in water content. *Scirpus* is intermediate between these species in water content and occupies intermediate positions on the scatter plot.

Fig. 5A demonstrates the interpolated spatial patterns in water content from the spectral continuum extracted from field spectra measured at the Mouth site. The locations of the field measurements used for interpolation estimates are shown on Fig. 5A. Canopy water displays a large absorption feature across the 900–1000 nm interval because of the high near-infrared reflectance of plants. Distinct narrow band features are not observed in open water, which has continuous low reflectance across the visible and near-infrared region. Because of this, the area measured under the continuum for open water is near zero. Thus, the patterns are due to variation in canopy water content and not surface water. These patterns closely match species distributions at this site. The shoreline is located along the bottom of the image and a microchannel along the top edge of the image, however the channel can not be distinguished easily from an interpolation at this scale.

The zone showing the lowest values of water content

TABLE 4. Correlation coefficients ($r$) between the indices and the biomass by species.

| Variable | VI | NDVI | SAVI | GEMI | ARVI | SARVI |
|---|---|---|---|---|---|---|
| *Salicornia virginica* | | | | | | |
| Green fresh mass | 0.71** | 0.53** | 0.52** | 0.43** | 0.73** | 0.58** |
| Green dry mass | 0.57** | 0.41** | 0.54** | 0.51** | 0.58** | 0.55** |
| *Scirpus robustus* | | | | | | |
| Green fresh mass | ns | ns | ns | ns | ns | ns |
| Green dry mass | ns | ns | ns | ns | ns | ns |
| *Spartina foliosa* | | | | | | |
| Green fresh mass | 0.61** | 0.64** | 0.71** | 0.54** | 0.61** | 0.73** |
| Green dry mass | 0.69** | 0.67** | 0.78** | 0.61** | 0.70** | 0.79** |

** $P < 0.01$, ns = not significant.

TABLE 5. Correlation coefficients ($r$) between the indices and the biomass by site and species.

| Variable | VI | NDVI | SAVI | GEMI | ARVI | SARVI |
|---|---|---|---|---|---|---|
| Mouth site, *Salicornia virginica,* $n = 26$ | | | | | | |
| Green fresh mass | 0.84** | 0.65** | 0.63** | 0.52** | 0.84** | 0.66** |
| Green dry mass | 0.81** | 0.66** | 0.67** | 0.58** | 0.82** | 0.71** |
| Mouth site, *Spartina foliosa,* $n = 9$ | | | | | | |
| Green fresh mass | 0.74** | 0.68** | 0.74** | 0.62* | 0.76** | 0.75** |
| Green dry mass | 0.72** | 0.67** | 0.73** | 0.63* | 0.74** | 0.75** |
| Pond site, *Salicornia virginica,* $n = 15$ | | | | | | |
| Green fresh mass | 0.81** | 0.77** | 0.75** | 0.64** | 0.80** | 0.78** |
| Green dry mass | 0.73** | 0.66** | 0.69** | 0.62** | 0.70** | 0.71** |
| River site, *Salicornia virginica,* $n = 15$ | | | | | | |
| Green fresh mass | ns | ns | 0.41* | 0.48* | ns | ns |
| Green dry mass | ns | ns | ns | ns | ns | ns |
| River site, *Spartina foliosa,* $n = 5$ | | | | | | |
| Green fresh mass | ns | 0.64* | 0.71* | ns | ns | 0.72* |
| Green dry mass | 0.86** | 0.84** | 0.89** | 0.69* | 0.86** | 0.91** |

*Note:* * $P < 0.05$; ** $P < 0.01$; ns = not significant.

(Fig. 5A) on the gray scale image (black), are dominated by *Spartina* along the shorelines and the microchannel. Near the top of the image is an interior drainage canal; the six black patches are located near the channel and represent low canopy water content *Spartina* stands. The lightest gray-white patches in the image are *Salicornia* and indicate patches of high canopy water content. *Salicornia* forms dense mats of 100% cover with near vertical fleshy green stems on the upper surface of the canopy. There is an east to west drying trend across the image corresponding to the water distribution across the marsh. The lower water content observed along the left side of the figure is at the location of a power utility catwalk (for access to high voltage power lines crossing the site). This site pattern in water content approximates the salinity and soil moisture gradients within this marsh.

Fig. 5B shows the estimated water content for the site derived from the airborne AVIRIS detected water absorption feature. The locations of the field measurements used for water content estimates are shown on Fig. 5B. Spatial patterns in water content closely approximate those created by IDW interpolation of the field measurements shown in Fig. 5A. Both Fig. 5A and B show lower water contents along the shoreline and along the left side of the image and an interior area of higher water content. The similarity in spatial patterns is evident although the actual water content estimates differ. The range of water contents is lower in the AVIRIS estimates, possibly a result of the scaling differences between the point and image data sets. The image estimates predict relatively more spatial area in the highest and lowest value ranges compared to the IDW estimates. Both figures show the east-to-west drying pattern. The left-to-right trending channel (near the top row of field samples) is observed to be continuous in the image data while it appears as separated patches from the interpolated point data. There is a continuous area of higher water content near the shoreline boundary of the *Salicornia* zone that appears as a more discrete area in the interpolated data. Finally, the interior levee (running along the upper edge of Fig. 5B) is beyond the edge of the interpolated data. These results demonstrate the feasibility of remote observation of landscape scale wetland condition estimates. They also illustrate the difficulty in extrapolating point data to larger landscape patterns.

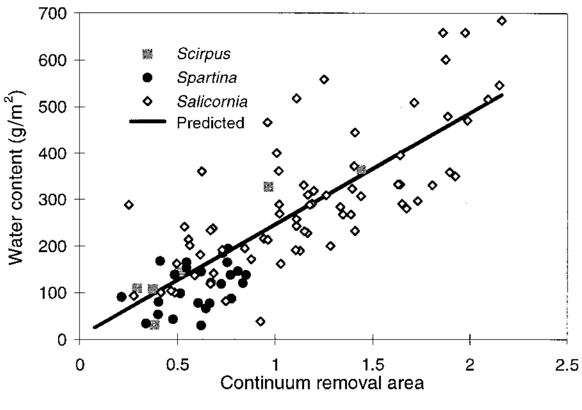

FIG. 4. The relationship between canopy water content (g/m²) and the area for the continuum removal (CRA) water absorption feature for salt marsh vegetation in San Pablo Bay, California, June 1994 (water content [g/m²] = 7.12 + 239.24 CRA, with $R^2$ = 63.3%).

### *Growth characteristics and edaphic factors*

To develop an understanding between growth and canopy reflectance within the marsh and relate these patterns to the spatial variation in edaphic factors we examined several canopy and soil properties. The canopy height varied significantly among species and sites (Table 6A). For *Salicornia,* the tallest plants were found at the Mouth site while plants at the Pond site were short and prostrate. *Salicornia* at the River site were

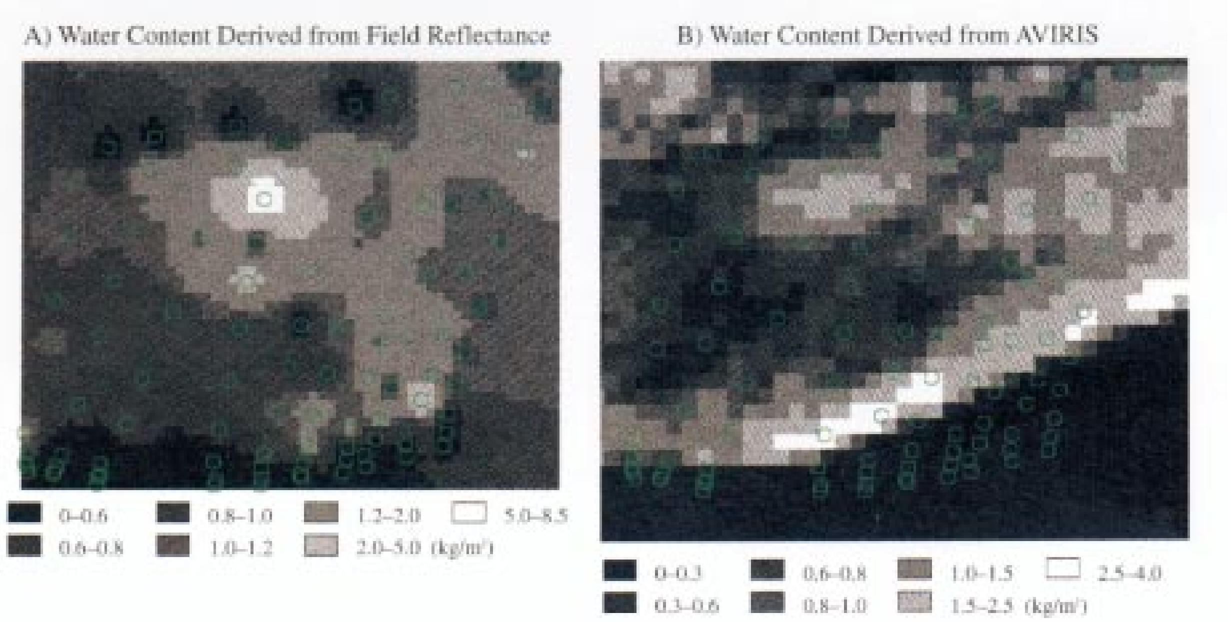

FIG. 5. (A) Spatial patterns of canopy water content interpolated from field reflectance at the Mouth site. The area shown is ≈300 by 380 m. Field sampling sites are indicated by green circles on the image. The water content is expressed as kg/m$^2$ with 10-m grid size. (B) Spatial patterns of canopy water content developed by regression from the spectral continuum removal method, applied to an area of an AVIRIS image corresponding to Fig. 5A. Field sampling sites are indicated by green circles on the image. The pixel size is 17.5 m.

intermediate in stature. For *Scirpus,* taller plants were found in the River site than the Mouth site and similar heights were found for *Spartina* at both sites. The LAI was similar at the Mouth and River sites for *Spartina,* and *Salicornia,* while LAI of *Salicornia* at the Pond site was significantly higher because plants were denser and had developed a higher proportion of photosynthetic growth at this site (Table 6A). LAI of *Scirpus* was greater at the Mouth site than at the River site. The difference in LAI may be due to the small number of *Scirpus* samples at the Mouth site.

Fig. 6 shows that *Salicornia* had similar aboveground (dry mass) biomass at the Mouth site and the Pond site, while the River site had much less biomass. Biomass at the Mouth and the Pond sites was significantly different from the River site at the 5% level. The dry mass of *Spartina* was significantly greater at the Mouth site than the River site. However, because of the presence of several species and therefore a wide range of biomass values at the Mouth and River sites, and the near exclusive dominance of the highly productive *Salicornia* at the Pond site, the Pond site showed the highest average site biomass (Fig. 6). The relative fresh mass water content for *Salicornia* was not statistically different at the three sites (Table 6A). The ratio of the canopy water mass to the dry mass was significantly linearly related to salinity among the sites and was highest at the River site and lowest at the Pond site ($r^2 = 0.98$). This decreasing trend in water content to increased dry mass between sites paralleled the increasing salinity among the sites.

The mean soil moisture content was highest at the Mouth and lowest at the Pond site (Table 6B). The average salinity level was lowest at the River site and highest at the Pond site following expected upstream and inland gradients (Fig. 7). Fig. 8 shows soil salinity and water contents as a function of distance from shoreline for these sites. Distance between points varies as indicated on the figure. Salinity generally increases sharply across the intertidal zone up to the mean high tide elevation and then remains at a high concentration across the high marsh, with exception for lower salinity in the vicinity of interior microchannels.

High concentrations of $H_2S$ were found along with high salinity and low soil moisture contents at the Pond site. Significantly less $H_2S$ was found in soils at the Mouth and River sites (Table 6B). Fig. 9 shows redox potential and $H_2S$ plotted as relative distance from the shoreline at the Mouth and River sites and distance from the pond at the Pond site. Redox is shown from both spatial averages as distance from shoreline and as diurnal averages at three distances. Redox and $H_2S$ were negatively correlated as were salinity and soil moisture (Fig. 8). Salinity and redox potentials increase with distance from river banks, microchannels, and the hypersaline pond, while soil moisture and $H_2S$ decline. These patterns are consistent with the frequency and duration of flooding between these sites.

The redox potential showed that the soil was more anoxic near the shoreline at the Mouth and River sites and values increased with distance from the shoreline (Fig. 9). The redox potential at M5 is low because it

TABLE 6. Data for the vegetation of three species at three sites and the environmental variables at three sites, June 1994.

A) Vegetation

| Location | Variables | *Salicornia* |  | *Spartina* |  | *Scirpus* |  |
|---|---|---|---|---|---|---|---|
|  |  | $\bar{X}$ | SE | $\bar{X}$ | SE | $\bar{X}$ | SE |
| Mouth | Canopy height, cm | 42 | 1.0 | 49 | 1.9 | 53 | 6.0 |
|  | LAI | 4.0 | 0.3 | 2.5 | 0.4 | 2.7 | 0.7 |
|  | Water content, % | 84 | 0.05 | 62.9 | 0.45 | 68.3 | 0.07 |
| Pond | Canopy height, cm | 27 | 1.8 | na |  | na |  |
|  | LAI | 5.5 | 0.5 | na |  | na |  |
|  | Water content, % | 80 | 0.10 | na |  | na |  |
| River | Canopy height, cm | 33 | 0.9 | 52 | 2.4 | 72 | 2.6 |
|  | LAI | 3.7 | 0.2 | 2.3 | 0.4 | 1.9 | 0.4 |
|  | Water content, % | 86.5 | 0.04 | 78.3 | 0.07 | 65.4 | 1.1 |

B) Environment

| Variables | Mouth |  | Pond |  | River |  |
|---|---|---|---|---|---|---|
|  | $\bar{X}$ | SE | $\bar{X}$ | SE | $\bar{X}$ | SE |
| Redox, mV | 282 | 85 | 157 | 69 | 251 | 55 |
| Hydrogen sulfide, mg/kg | 4.8 | 1.3 | 75.5 | 10.0 | 5.2 | 1.5 |
| Salinity, g/kg | 27.6 | 1.1 | 41.0 | 1.5 | 22.0 | 0.9 |
| Soil moisture, % | 87.7 | 4.5 | 36.5 | 11.3 | 76.5 | 6.8 |
| N total, mg/kg | 0.192 | 0.005 | 0.610 | 0.053 | 0.292 | 0.056 |
| $NH_4$-N in water, mg/kg | 0.722 | 0.1 | 6.848 | 0.567 | 0.406 | 0.066 |
| $NO_3$-N in water, mg/kg | 0.036 | 0.005 | 0.106 | 0.012 | 0.157 | 0.008 |
| $NH_4$-N in soil, mg/kg | 2.354 | 0.242 | 25.806 | 3.595 | 1.827 | 0.148 |
| $NO_3$-N in soil, mg/kg | 0.079 | 0.01 | 0.024 | 0.005 | 1.824 | 0.117 |

*Note:* Data are mean ± 1 standard error, na = not available.

was located along an interior channel. The redox potentials at the Pond site were significantly lower and values did not change consistently with distance from the pond. Redox potentials temporally vary with tidal cycle. Mean diurnal measurements made at three points in each site nonetheless, showed similar redox potential relationships as seen with spatial averages both within and between sites. Diurnal averages at the Mouth and Pond sites were higher than the one-time spatial averages, suggesting that the spatial samples were obtained when the soil moisture was near maximum saturation.

Total soil nitrogen paralleled this pattern with the Mouth site having the least nitrogen and the Pond site the most nitrogen. Significantly more $NH_4$-N was found than $NO_3$-N in both interstitial water and soil extracts at all three sites due to the reducing conditions (Fig. 10). Relatively higher $NO_3$-N was present at the River site than at the other sites (Table 6B). Fig. 11 shows the relationship between distance from shoreline and soil and water $NH_4$-N and $NO_3$-N concentrations. Ammonium nitrogen was significantly higher at the Pond site. Much larger ratios of $NH_4$-N to $NO_3$-N were found at the Pond site (64.3 in water and 1062 in soil) and smaller ratios at the River site. The ratio of $NH_4$-N to $NO_3$-N was 20.1 in water and 29.8 in soil at the Mouth

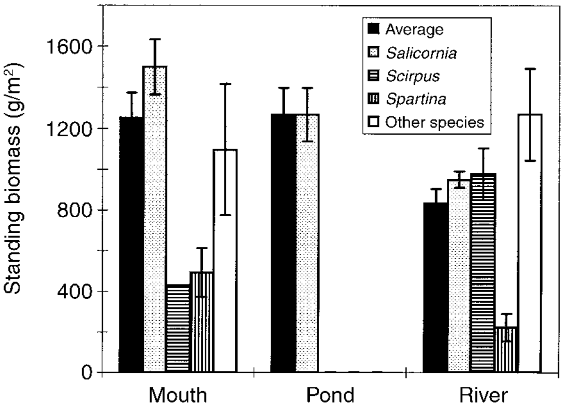

FIG. 6. Dry biomass of the three species (*Salicornia virginica, Spartina foliosa,* and *Scirpus robustus*) from three study sites in San Pablo Bay salt marsh, California, June 1994. The biomass of individual species is expressed as the average of the sampled points of that species. The ''average'' bar represents the mean biomass of all samples at the study site. Error bars indicate ±1 SE.

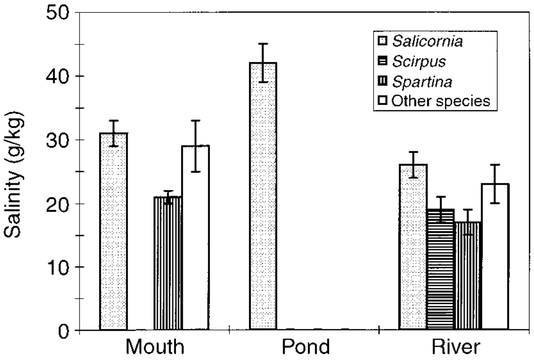

FIG. 7. Mean interstitial water salinity (g/kg) in species zones at the three study sites. Error bars indicate ±1 SE.

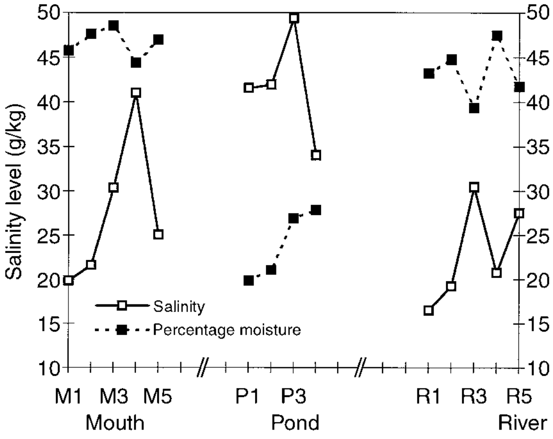

FIG. 8. Soil salinity and percentage of soil moisture change measured from the shoreline to inland at Mouth and River sites and moving away from the pond at the Pond site. Distances from the shoreline of R1, R2, R3, R4, and R5 are ~15, 30, 60, 90, and 120 m, respectively; distances from the shoreline of M1–M5 are ~20, 30, 50, 170, and 320 m. The distances from the hypersaline pond of P1–P4 are 0, 15, 30, and 60 m.

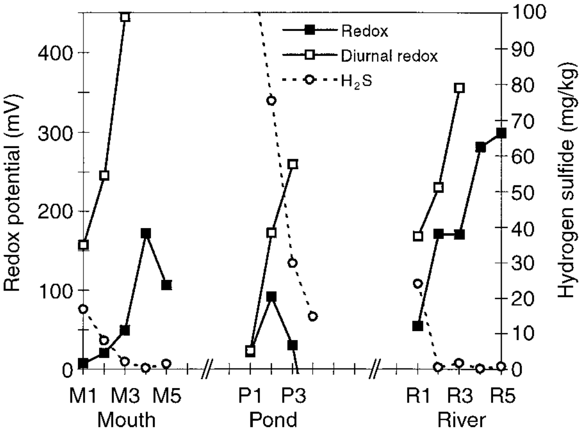

FIG. 9. Redox potential and hydrogen sulfide concentrations from the shoreline to inland at Mouth and River sites and moving away from the pond at the Pond site. Distances from the shoreline of R1, R2, R3, R4, and R5 are ~15, 30, 60, 90, and 120 m, respectively; distances from the shoreline of M1–M5 are ~20, 30, 50, 170, and 320 m. The distances from the hypersaline pond of P1–P4 are 0, 15, 30, and 60 m.

site. It was obvious from these results that $NH_4$-N is positively correlated with $H_2S$ and other nutrients.

Canopy height was not correlated with biomass at any of the sites or for any of the species, although it generally decreased with salinity. Height was more closely associated with the woody biomass. LAI was strongly correlated with green biomass ($r = 0.99$). Higher biomass was associated with high nutrients, especially $NH_4$-N, but no strong relationship was found between $NO_3$-N and standing biomass. However, salin-

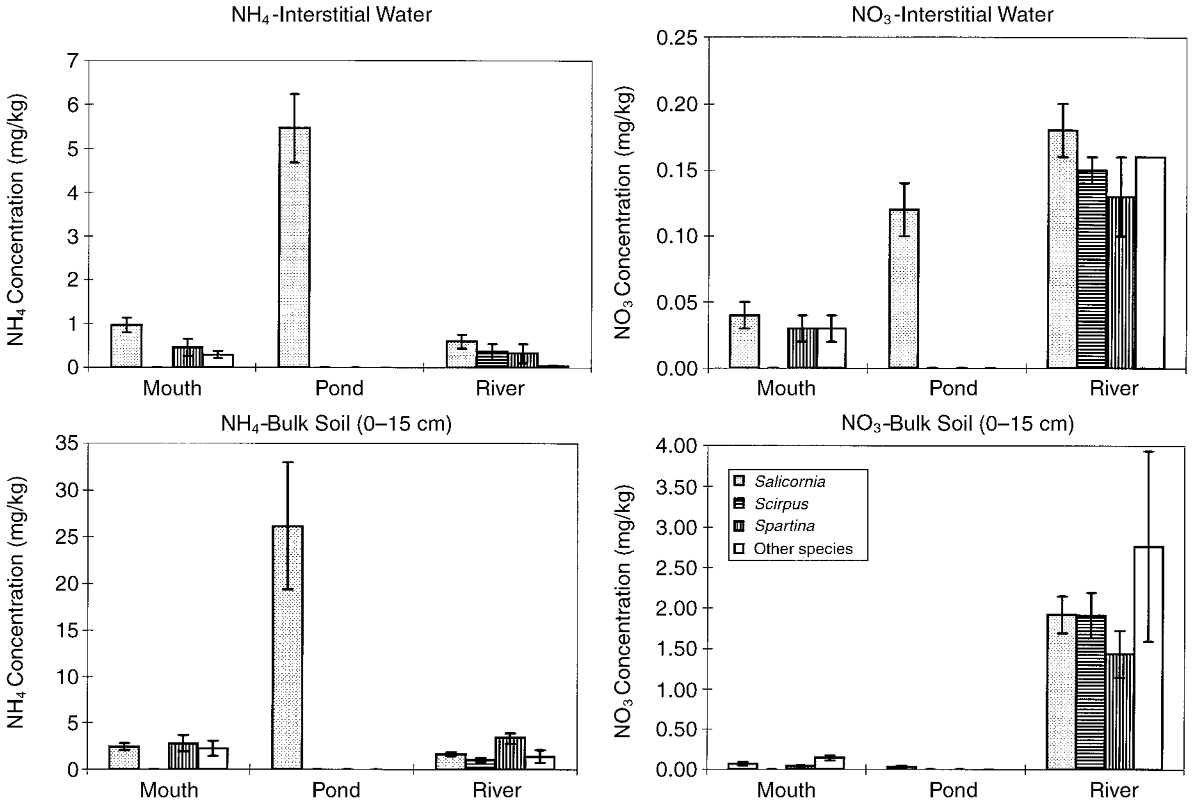
$NH_4$-Interstitial Water

$NO_3$-Interstitial Water

$NH_4$-Bulk Soil (0–15 cm)

$NO_3$-Bulk Soil (0–15 cm)

FIG. 10. Nitrogen concentrations in the interstitial water and soils at the three sites. Error bars indicate ±1 SE.

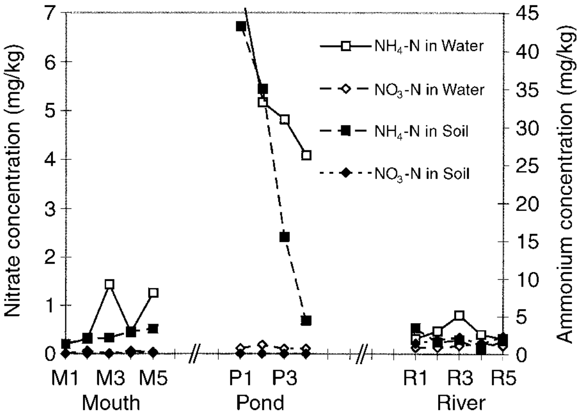

FIG. 11. Nitrogen concentration change from the shoreline to inland at Mouth and River sites and moving away from the pond at the Pond site. Distances from the shoreline of R1, R2, R3, R4, and R5 are ~15, 30, 60, 90, and 120 m, respectively; distances from the shoreline of M1–M5 are ~20, 30, 50, 170, and 320 m. The distances from the hypersaline pond of P1–P4 are 0, 15, 30, and 60 m.

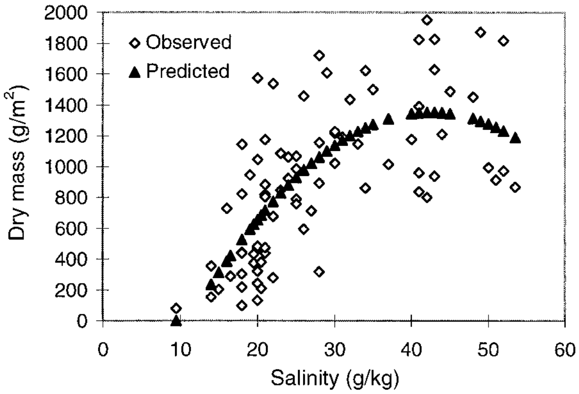

FIG. 12. The relationship between canopy dry mass (g/m$^2$) and salinity levels (g/kg) in interstitial water in San Pablo Bay marshes, California, June 1994 (dry mass [g/m$^2$] = $-1127.72 + 116.46$ g/kg $- 1.37$ [g/kg]$^2$, with $R^2$ = 49%).

ity significantly affects standing biomass in these marshes. Forty-nine percent of the variation in total dry mass can be explained by salinity for *Salicornia* (Fig. 12).

## DISCUSSION

Since canopy reflectance is an integrated measure of canopy characteristics, species differences expressed in standing biomass and water content should be recorded in the canopy spectra (Baret and Guyot 1991). Because reflectance differences between the species in the visible and infrared regions of the electromagnetic spectrum relate primarily to pigment and water absorption features, we expected that differences in green biomass and water content would be detectable. Previous research has shown that biomass can be predicted from spectral vegetation indices in forest/pasture, agricultural crops, aquatic plants, and salt marshes (Drake 1976, Hardisky et al. 1986, Lozano-Garcia et al. 1991, Gross et al. 1993, Penuelas et al. 1993). We found that canopy biomass could be estimated using remotely sensed spectral vegetation indices at 58–80% accuracy depending on species. This is comparable to the 65% reported by Gross et al. (1993) for *Typha* biomass using a simple VI. Furthermore, most indices provided significant correlations with canopy variables and relative trends consistent with edaphic gradients.

Biomass and LAI were highly correlated ($r^2 = 0.99$), which possibly allows the use of remotely sensed vegetation indices based on foliar pigment absorption and LAI. *Spartina* and *Scirpus* had lower LAI and percent cover than *Salicornia,* and therefore, more of the soil and litter components contributed to the canopy spectrum. The nearly double LAI in *Salicornia* compared to *Scirpus* and *Spartina* was due to the dense erectophile foliage distribution of the canopy. Because of the low LAI in *Spartina* and *Scirpus,* SAVI better described the vegetation characteristics than VI since variation in the soil component was minimized. These results suggested that if it were possible to map species distributions first, it would be best to use the VI to predict standing biomass for *Salicornia,* and SAVI to estimate biomass for *Spartina* and *Scirpus.*

Because *Salicornia* dominated the marsh with almost full cover at all sampling points, ARVI and SARVI should have been the best indices to maximize the vegetation measure while minimizing differences in optical density of the atmosphere at different sun angles (Kaufman and Tanre 1992, Huete et al. 1994). Nonetheless, VI had correlation coefficients nearly as good as ARVI, and so did SAVI when compared to SARVI (Tables 4 and 5). We infer that correcting for atmospheric effects may not be necessary in these marshes during the early summer when the sky is clear and relative humidity is low. However, SAVI would be the better index to select for prediction of biomass when soil exposure is high relative to the percentage canopy cover.

TM data of the area were displayed as a gray scale VI image (Fig. 1). Clearly, spatial patterns evident within the marsh were consistent with patterns of biomass abundance. Gradients from the river margin are apparent at the Mouth and River sites. Significant spatial variation exists in the extensive marsh that includes the Pond and River sites. Although the patterns outside our study sites were not validated in careful detail, these results support the use of remote sensing to map biomass distributions in California salt marshes. Sites in the image with high VI values are agricultural fields, planted in small grains.

By June, most *Salicornia* had developed full canopy cover at all three study sites while *Spartina* and *Scirpus* had incomplete canopy cover. The distribution of these species was inferred from the zonation patterns observed by the gray scale variation in the TM scene (Fig. 1). The best time to measure canopy reflectance would be near the summer solstice when sun angles are highest and peak summer growth has been achieved.

The decline in canopy water content coincided with increasing soil salinity and decreasing water content within and between sites. The site trend was largely driven by canopy differences in *Salicornia.* These results are consistent with a greenhouse study on water content and salt accumulation in 19 genera of succulent halophytes (Glenn and O'Leary 1984), which found that water content increased up to an external salinity of 10.5 g/kg but declined at higher salinities and was related to ability to maintain shoot osmotic potentials. Briens and Larher (1982) also found a strong correlation between water content and mineral uptake in 15 salt marsh species growing under a range of marsh conditions. Thus, the canopy water content appears to be a good indicator of soil salinity and species adjustment to external osmotic potentials.

Moreover, because species differ in water content, the dominant salt marsh species can be spectrally differentiated by their water absorption features. We compared the predicted canopy water content as estimated from the spectral water feature and ratioed it to the VI (an estimate for dry mass biomass). The coefficient of determination for the regression between the spectrally determined ratio and the directly measured water content to dry mass ratio was $r^2 = 0.84$. These results indicate that the water content measure and the VI were not measuring the same canopy property, so one can use spectral information to independently estimate both water content (as an indicator of osmotic adjustment) and biomass.

The water feature relationship can be used to predict the spatial variation in canopy water content in salt marshes using a remotely sensed image of the 970-nm water band. Current Landsat satellites cannot measure this band but the next generation of earth-observing satellites (e.g., the Lewis sensor), will be capable of such measurements. Such physiological measures could be important to understanding responses to salinity and osmotic adjustment in these communities or to phenological changes. This technique could be used to distinguish community zonation without requiring substantial calibration from field observations.

Zonal relationships in physical variables within these salt marshes are repeated over extended time periods despite the dynamic range of species distributions and edaphic conditions due to short-term inter- and intra-annual processes. Salinity often controls zonation patterns and marsh productivity (Atwater and Hedel 1976, Mahall and Park 1976, Ustin et al. 1982, Whitlow 1982, Mitsch and Gosselink 1993). Salinity was lowest in the intertidal (*Spartina*) zone paralleling the shoreline and increased with elevation and distance inland at both Mouth and River sites (*Salicornia* zone). At the Pond site, salinity initially increased with distance from the ponds and then decreased beyond a zone of effect (Fig. 8). Because the Pond site is located around a hypersaline pond, soil salinity is higher than at the other two sites and growth is restricted to *Salicornia.* The Pond site receives less fresh water influx and our long term observations show that interstitial water salinity at that site has ranged from 24 to 78 g/kg (E. Rejmankova, *unpublished data*). Thus, mapping species distributions and variations in biomass can provide inferences about the edaphic conditions controlling the patterns.

Salinity and soil water content were negatively correlated. Consistent with these edaphic patterns, large differences were also found in N, P, and S between sites and within sites with the lowest concentrations found in the intertidal zone and significantly higher concentrations in the upper marsh. The patterns we found in Eh, soil moisture, salinity, and plant growth are consistent with observations by Whitlow (1982) and indicate more reduced conditions in the lower marsh where plant growth is less and the Pond site where hypersaline conditions are found. High Eh values have been observed within the root zone where plants were actively growing and low values below the root zone and in bare soil patches (Linthurst and Seneca 1980, Howes et al. 1981).

The availability of nitrogen in the marsh is important for the productivity of the salt marsh ecosystem (Covin and Zedler 1988, DeLaune et al. 1989). The Pond site had the highest mean biomass, total nitrogen, and also the highest $NH_4$-N among all the sites. Higher $NH_4$-N at the Pond site may have resulted because of high salinity, nitrogen excess, and soil decomposition conditions. As found for spatial distribution of soil nutrients and salinity, organic matter was highest in the upper marsh and lowest in the lower intertidal region. This pattern apparently results from both higher biomass turnover in the *Salicornia* zone and the lesser tidal transport in the upper marsh. Recent reports have indicated the possibility of direct measurement of canopy nitrogen content and litter using hyperspectral data (Jacquemoud et al. 1996; J. E. Pinzon et al., *unpublished manuscript*; D. A. Roberts et al., *unpublished manuscript*).

The distribution of these species, their aboveground biomass, and the canopy water content were indicative of the mean salinity and soil moisture levels and the magnitude of seasonal variation. Whether any of these spectral indices eventually could be used to infer edaphic conditions and/or canopy height or surface roughness is uncertain and requires further research. However, the correlations suggest that it may be possible to indirectly detect an integrated measure of soil salinity, soil moisture, and nitrogen using various remote sensing techniques sensitive to canopy properties. Although these species responded to salinity through quite different physiological mechanisms, all show growth declines after salinity reaches a threshold above seawater concentration.

## CONCLUSIONS

Our study integrates remote sensing and field data to examine the ecology of the salt marsh and the spatial distribution of physical and biological processes. Significant spatial variability in soil and interstitial water salinity, nitrogen, and redox potential was found in San Pablo Bay salt marshes. These marshes were dominated by *Salicornia* for all regions above mean high tide; nonetheless, significant variation in plant distribution and growth reflected site edaphic conditions. Higher species diversity was found closer to the channels and at sites with low salinity. These microchannels provide renewed sources of water and nutrients for parts of the marshes at some distance from a main tidal channel. Standing biomass of the three species was influenced by several correlated environmental factors, including salinity, soil moisture, redox potential, and $H_2S$. Soil salinity did not limit plant growth in *Salicornia* up to 42 g/kg while *Spartina* and *Scirpus* growth was limited at much lower levels. Ammonium nitrogen was the predominant form of available nitrogen in the soil and was positively related to increased plant growth.

Green fresh biomass and related variables were estimated using spectral vegetation indices. Species differences were not apparent in vegetation indices. Despite the fact that better predictions of *Spartina* biomass were obtained using a Soil Adjusted Vegetation Index and *Salicornia* biomass using a simple Vegetation Index, indices provided significant fits to all data. Moreover, any of the spectral vegetation indices can be used to estimate standing biomass in these salt marshes. This suggests that reasonable spatial estimates can be obtained regardless of measurement condition or species composition. Incomplete canopy cover and high proportion of woody stem/litter components resulted in differences among indices. Thus, under low cover classes, an index like SAVI that accounts for the spectral contribution of soil is best. At the other extreme, when cover is high, VI saturates and an index that has more sensitivity at high LAI improves the fit.

Lastly, canopy condition can be estimated using a spectral estimate of water absorption. Sanderson et al. (*unpublished manuscript*) have examined the scaling changes between field-measured canopy water content and water content predicted from AVIRIS images over this marsh. The close correspondence they show supports the potential for mapping canopy water content from airborne or satellite observations at synoptic scales. Such information could be useful in monitoring osmotic conditions and adjustment in salt marshes species. Based on reflectance differences, the three dominant species may be differentiated using this information and species zonations may be mapped using AVIRIS images (Zhang et al. 1996). Such spectral identifications can be done sequentially, providing the optimal test for separating each of the most common marsh species. Therefore, we believe that the use of hyperspectral remote sensing technologies to monitor the ecological conditions, salt marsh species distributions, and dynamic changes over time is promising.

## ACKNOWLEDGMENTS

We thank Claudia Castaneda, Larry Costick, Martha Diaz, Quinn Hart, Robert Haxo, Kent Jorgensen, Jorge Pinzon, Rebecca Post, George Scheer, Harry Spengler, Lai-Han Szeto, Linette Young, Gail Wheeler, and Qingfu Xiao for help in conducting the field measurements for this research and to Quinn Hart for assistance with the TM image. We thank Yaffa Grossman and Jon Syder for helpful comments on an earlier draft of the manuscript. We wish to recognize the support of the U.S. Environmental Protection Agency grant R82-1695-010 and the NASA EOS program under grants NAS5-31359 and NAS5-31714, and to the Sequoia 2000 grant from the Digital Equipment Corporation that provided DEC 5000 and Alpha 3000 workstations and peripherals that were used to perform this research.

## LITERATURE CITED

Allen, S. E., editor. 1989. Chemical analysis of ecological materials. Second edition. Blackwell Scientific, Oxford, England.

Atwater, B. F., S. G. Conard, J. N. Dowden, C. W. Hedel, R. L. MacDonald, and W. Savage. 1980. History of land forms and vegetation of the estuary's tidal marshes in San Francisco Bay. Pages 347–384 *in* T. J. Conomos, editor. The urbanized estuary. Pacific Division American Association for the Advancement of Science, San Francisco, California, USA.

Atwater, B. F., and C. W. Hedel. 1976. Distribution of seed plants with respect to tide levels and water salinity in the natural tidal marshes of the northern San Francisco Bay estuary, California. U.S. Geological Survey open file report **76–389**.

Baret, F., and G. Guyot. 1991. Potentials and limits of vegetation indices for LAI and APAR assessment. Remote Sensing of the Environment **35**:161–173.

Bertness, M. D., and A. M. Ellison. 1987. Determinations of pattern in a New England salt marsh plant community. Ecological Monographs **57**:129–147.

Briens, M., and F. Larher. 1982. Osmoregulation in halophytic higher plants: a comparative study of soluble carbohydrates, polyols, betaines and free proline. Plant, Cell and Environment **5**:287–292.

Christensen, S., and J. Goudriaan. 1993. Deriving light interception and biomass from spectral reflectance ratio. Remote Sensing of Environment **43**:87–95.

Clark, R. N., and T. L. Roush. 1984. Reflectance spectroscopy: Quantitative analysis techniques for remote sensing applications. Journal of Geophysics Research **89**(B7): 6329–6340.

Covin, J. D., and J. B. Zedler. 1988. Nitrogen effects on *Spartina foliosa* and *Salicornia virginica* in the salt marsh at Tijuana estuary, California. Wetlands **8**:51–65.

CSES/CIRES. 1996. Atmosphere REMoval Program (ATREM) User's Guide. Version 2.0. Center for the Study of Earth from Space (CSES), Cooperative Institute for Research in Environmental Sciences (CIRES), University of Colorado, Boulder, Colorado, USA.

DeLaune, R. D., T. C. Feijtel, and W. H. Patrick, Jr. 1989. Nitrogen flows in Louisiana Gulf Coast salt marsh: Spatial considerations. Biogeochemistry **8**:25–37.

Deleeuw, J., H. Olff, and J. P. Bakker. 1990. Year-to-year variation in peak above-ground biomass of six salt marsh angiosperm communities as related to rainfall deficit and inundation frequency. Aquatic Botany **36**:139–151.

Drake, B. G. 1976. Seasonal changes in reflectance and standing crop biomass in three salt marsh communities. Plant Physiology **58**:696–699.

Glenn, E. P., and J. W. O'Leary. 1984. Relationship between salt accumulation and water content of dicotyledonous halophytes. Plant, Cell and Environment **7**:253–261.

Goel, N. S. 1988. Models of vegetation canopy reflectance and their use in estimation of biophysical parameters from reflectance data. Remote Sensing Reviews **4**:1–212.

Gross, M. F., M. A. Hardisky, and V. Klemas. 1989. Applications to the coastal wetlands vegetation. Page 734 *in* G. Asrar, editor. Theory and applications of optical remote sensing. Wiley Series in Remote Sensing, New York, New York, USA.

Gross, M. F., M. A. Hardisky, P. L. Wolf, and V. Klemas. 1993. Relationship among *Typha* biomass, pore water methane, and reflectance in a Delaware (U.S.A.) brackish marsh. Journal of Coastal Research **9**:339–355.

Gross, M. F., and V. Klemas. 1986. The use of airborne imaging spectrometer (AIS) data to differentiate marsh vegetation. Remote Sensing of the Environment **19**:97–103.

Hager, S. W., and L. E. Schemel. 1992. Sources of nitrogen and phosphorus to Northern San Francisco Bay. Estuaries **15**:40–52.

Hardisky, M. A., M. F. Gross, and V. Klemas. 1986. Remote sensing of coastal wetlands. Bioscience **36**:453–460.

Hardisky, M. A., R. M. Smart, and V. Klemas. 1983. Seasonal spectral characteristics and aboveground biomass of the tidal marsh plant, *Spartina alterniflora.* Photogrammetric Engineering and Remote Sensing **49**:85–92.

Howes, B. L., R. W. Howarth, J. M. Teall, and I. Valiela. 1981. Oxidation-reduction potentials in a salt marsh: Spatial patterns and interactions with primary production. Limnological Oceanography **26**:350–360.

Huete, A. C. 1988. A soil adjusted vegetation index (SAVI). Remote Sensing of the Environment **17**:37–53.

Huete, A., C. Justice, and H.Liu. 1994. Development of vegetation and soil indices for MODIS-EOS. Remote Sensing of the Environment **49**:224–234.

Ibarra-Obando, S. E., and M. Poumian-Tapia. 1992. The saltmarsh vegetation of Punta Banda Estuary, Baja California, Mexico. Pages 201–212 *in* U. Seeliger, editor. Coastal plant communities of Latin America. Academic Press, San Diego, California, USA.

Jacquemoud, S., S. L. Ustin, J. Verdebout, G. Schmuck, G. Andreoli, and B. Hosgood. 1996. Estimating leaf biochemistry using the PROSPECT leaf optical properties model. Remote Sensing of the Environment **56**:194–202.

Kaufman, Y. J., and D. Tanre. 1992. Atmospherically resistant vegetation index (ARVI) for EOS-MODIS. IEEE Transactions in Geoscience and Remote Sensing **30**:261–270.

Klemas, V. V., J. E. Dobson, R. L. Ferguson, and K. D. Haddad. 1993. A coastal land cover classification system for the NOAA coastwatch change analysis project. Journal of Coastal Research **9**:862–872.

Leibowitz, N. C., and M. T. Brown. 1990. Indicator strategies for wetlands. Pages 5.1–5.15 *in* C. T. Hunsaker and D. E. Carpenter, editors. EMAP ecological indicators. EPA/600/3-90/060, Environmental Protection Agency, Washington, D.C., USA.

Linthurst, R. A., and E. D. Seneca. 1980. The effects of standing water and drainage potential on the *Spartina alterniflora*-substrate complex in a North Carolina salt marsh. Estuarine and Coastal Marine Science **11**:41–52.

Lozano-Garcia, D. F., R. N. Fernandez, and C. J. Johannsen. 1991. Assessment of regional biomass–soil relationships using vegetation indexes. IEEE Transactions on Geoscience and Remote Sensing **29**:331–339.

Mahall, B. E., and R. B. Park. 1976. The ecotone between *Spartina foliosa* trin. and *Salicornia virginica* L. in salt marshes of Northern San Francisco Bay, I. Biomass and production. Journal of Ecology **64**:421–433.

McKee, K. L., I. A. Mendelssohn, and M. Hester. 1988. Reexamination of pore water sulfide concentrations and redox potentials near aerial roots of *Rhizophora mangle* and *Avicennia germinans.* American Journal of Botany **75**:1352–1359.

Mitsch, W. J., and J. G. Gosselink. 1993. Wetlands. Van Nostrand Reinhold, New York, New York, USA.

Myneni, R. B., and D. L. Williams. 1994. On the relationship between FAPAR and NDVI. Remote Sensing of the Environment **49**:200–211.

Norman, J. M., and G. S. Campbell. 1989. Canopy structure. Pages 301–326 *in* R. W. Pearcy, J. Ehlringer, H. A. Mooney, and P. W. Rundel, editors. Plant physiological ecology, field methods and instrumentation. Chapman and Hall, New York, New York, USA.

Odum, E. P. 1983. Basic ecology. Saunders, Philadelphia, Pennsylvania, USA.

Pearcy, R. W., and S. L. Ustin. 1984. Effects of salinity on growth and photosynthesis of three California tidal marsh species. Oecologia **62**:68–73.

Pearson, R. L., and L. D. Miller. 1972. Remote mapping of standing crop biomass for estimation of the productivity of the short-grass Prairie, Pawnee National Grasslands, Colorado. Pages 1357–1381 *in* Proceedings 8th International Symposium on Remote Sensing of Environment, ERIM, Ann Arbor, Michigan, USA.

Penuelas, J., J. A. Gamon, K. L. Griffin, and C. B. Field. 1993. Assessing community type, plant biomass, pigment composition, and photosynthetic efficiency of aquatic vegetation from spectral reflectance. Remote Sensing of the Environment **46**:110–118.

Pinty, B., and M. M. Verstraete. 1992. GEMI: a non-linear index to monitor global vegetation from satellites. Vegetatio **101**:15–20.

Roughgarden, J., S. W. Running, and P. A. Matson. 1991. What does remote sensing do for ecology? Ecology **72**:1918–1922.

Rouse, J. W., R. H. Haas, J. A. Schell, D. W. Deering, and J. C. Harlan. 1974. Monitoring the vernal advancement of retrogradation of natural vegetation. NASA/GSFC, Type III, Final Report, NASA Goddard Space Flight Center, Greenbelt, Maryland, USA.

SAS. 1990. Statistical manual. SAS Institute, Cary, North Carolina, USA.

Ustin, S. L., R. W. Pearcy, and D. E. Bayer. 1982. Plant water relations in a San Francisco Bay salt marsh. Botanical Gazette **143**:368–373.

Whitlow, T. H. 1982. Plant–soil interactions in a San Francisco Bay salt marsh. Dissertation. University of California, Davis, California, USA.

Zedler, J. B. 1983. Freshwater impacts in normally hypersaline marshes. Estuaries **6**:346–355.

Zhang, M., J. Pinzon, S. L. Ustin, and E. Rejmankova. 1996. Differentiating salt marsh species using foreground/background analysis. Proceedings of ERIM Second International Airborne Remote Sensing Conference. 24–28 June 1996, San Francisco, California, USA.